

diffused out from the support. Thus our experimental results are consistent with the decoration model rather than the pillbox model.

Finally, we believe that the present results demonstrate the potential use of the analysis of the temperature dependence of EXAFS even in the case of a relatively complicated system like

supported metal catalysts.

Acknowledgment. We express our thanks to Dr. Nobuhiro Kosugi for his advice and stimulating discussion.

Registry No. Pt, 7440-06-4; Rh, 7440-16-6; TiO₂, 13463-67-7.

Surface Chemistry of C-N Bonds on Rh(111). 1. C₂N₂ and CH₃NH₂

S. Y. Hwang, A. C. F. Kong, and L. D. Schmidt*

Department of Chemical Engineering and Materials Science, University of Minnesota, Minneapolis, Minnesota 55455 (Received: January 23, 1989; In Final Form: June 9, 1989)

The adsorption and decomposition of C₂N₂ and CH₃NH₂ on Rh(111) have been studied by using temperature-programmed desorption (TPD) and Auger electron spectroscopy (AES). Both molecules adsorb readily on Rh(111) at 300 K and totally decompose. At very low coverages, C₂N₂ decomposes completely to N₂ (desorbing at 820 K) and surface carbon residues, while at saturation coverage (6.7 × 10¹⁴ molecules/cm²), ~80% of C₂N₂ desorbs intact and 20% of C₂N₂ decomposes to N₂ and surface carbon. Adsorption of CH₃NH₂ at 300 K produces H₂ and N₂ as major products at low coverages. Almost equal amounts of N₂ (10%), C₂N₂ (9%), and HCN (7%) are produced with H₂ (74%) at saturation coverage. CH₃NH₂ is totally dehydrogenated by 500 K to leave surface CN which then follows the same decomposition path as C₂N₂. The saturation density is ~8.2 × 10¹⁴ CH₃NH₂ molecules/cm² at 300 K. The chemistry of the C-N bonds in C₂N₂ and CH₃NH₂ is therefore similar in that 20% (in C₂N₂) and 39% (in CH₃NH₂) of the bond is cleaved to produce N₂ and surface carbon residues while the rest desorbs intact as HCN and C₂N₂. Their reactivities and selectivities on Rh(111) are much higher than those on Pt(111) where no C-N bond cleavage occurs and lower than Ni where total C-N bond cleavage is observed.

Introduction

It is becoming evident that group VIII transition metals have large variations in their ability to break the C-N bond, with Pt yielding no dissociation and Ni producing complete dissociation. Rh is intermediate in adsorption properties, and its selectivity in C-N bond dissociation should therefore be instructive in interpreting bond-breaking processes.

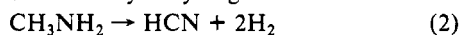
Interest in CN and CNO bond surface chemistry derives from many industrial reactions such as synthesis of HCN from CH₄, NH₃, and O₂ over Pt-Rh gauzes (the Andrussov process). These systems have been studied much less than C-O bond systems, and, as is shown from this work, CNO bond chemistry is much more selective on noble metals than are CO bonds.

Recently, we investigated the adsorption and decomposition of CH₃NH₂¹ and CH₃NO₂ and C₂N₂² on Pt(111) using TPD, AES, and XPS. We found that C-N bonds in all three molecules are very stable on Pt(111) in that no significant C-N bond scission (identified by N₂ formation) is observed in TPD up to 1250 K. Investigation of the decomposition and oxidation of CH₃NH₂ on polycrystalline Pt wires³ at higher pressures (0.5-10 Torr) also revealed that the addition of oxygen over Pt wires at 1450 K did not significantly change the decomposition chemistry of C-N bonds in CH₃NH₂ until oxygen was in excess.

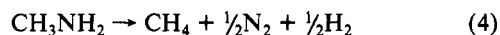
In this study, we use TPD and AES to examine the adsorption and decomposition of C₂N₂ and CH₃NH₂ on Rh(111). Cyanogen should desorb intact or decompose by C-N bond scission



which leaves carbon residues on the metal surface. Methylamine decomposition should occur by dehydrogenation



or by C-N bond breaking



which can also yield NH₃ and surface carbon residues.

The adsorption and decomposition of C₂N₂ on clean metal surfaces has been investigated previously on Pt(111),^{2,4,5} Pt(110),⁶ Pt(100),⁷ Rh(111),⁸ Pd(111),^{9,10} Pd(100),¹⁰ Ni(111),¹¹ Cu(111),^{12,13} Cu(110),¹⁴ Ag(110),¹⁵ and Ru(100).¹⁶ On Ag(110) C₂N₂ adsorbs only molecularly. It adsorbs dissociatively (as CN_{ad}) and desorbs as C₂N₂ through recombination of CN radicals in TPD on Pt, Pd, and Cu surfaces. On Ru(111) it adsorbs dissociatively and decomposes partially to N₂ and surface C upon heating. On Ni(111) it adsorbs dissociatively and decomposes completely to N₂ and surface carbon species upon TPD.

C₂N₂ thermal desorption on Pt(111) has been studied in detail in this laboratory.² C₂N₂ adsorbed on Pt(111) at 300 K produces at least five desorption peaks at 380 (α), 710 (γ), 810 (β₁), 910 (β₂), and ~1100 K (β₃), in which the α state was attributed to molecularly adsorbed C₂N₂, the γ state as the "polymeric state", and the β states as associative desorption of surface CN. No C-N

(4) Kingsley, J. R.; Dahlgren, D.; Hemminger, J. C. *Surf. Sci.* **1984**, *139*, 417.

(5) Hoffmann, W.; Bertel, E.; Netzer, F. P. *J. Catal.* **1979**, *60*, 316.

(6) Bridge, M. E.; Lambert, R. M. *Surf. Sci.* **1977**, *63*, 315.

(7) Conrad, H.; Kuppers, J.; Nitschke, F.; Netzer, F. P. *Chem. Phys. Lett.* **1977**, *46*, 571.

(8) Solymosi, F.; Bugyi, L. *Surf. Sci.* **1984**, *147*, 685.

(9) Kordes, M. E.; Stenzel, W.; Conrad, H. *J. Electron Spectrosc. Relat. Phenom.* **1986**, *39*, 89.

(10) Kordes, M. E.; Stenzel, W.; Conrad, H. *Surf. Sci.* **1987**, *186*, 601.

(11) Hemminger, J. C.; Muettteries, E. L.; Somorjai, G. A. *J. Am. Chem. Soc.* **1979**, *101*, 62.

(12) Solymosi, F.; Kiss, J. *Surf. Sci.* **1981**, *108*, 368.

(13) Kordes, M. E.; Stenzel, W.; Conrad, H.; Weaver, M. J. *J. Am. Chem. Soc.* **1987**, *109*, 1878.

(14) Outka, D. A.; Jorgensen, S. W.; Friend, C. M.; Madix, R. J. *J. Mol. Catal.* **1983**, *21*, 375.

(15) Bridge, M. E.; Marbrow, R. A.; Lambert, R. M. *Surf. Sci.* **1976**, *57*, 415.

(16) Gudde, N. J.; Lambert, R. M. *Surf. Sci.* **1983**, *124*, 372.

(1) Hwang, S. Y.; Seebauer, E. G.; Schmidt, L. D. *Surf. Sci.* **1987**, *188*, 21.

(2) Hwang, S. Y.; Kong, A. C. F.; Schmidt, L. D., submitted for publication in *Surf. Sci.*

(3) Hwang, S. Y.; Schmidt, L. D. *J. Catal.* **1988**, *114*, 230.

bond scission or nitrogen desorption was observed on Pt(111). The saturation density at 300 K was estimated to be $\sim 3.0 \times 10^{14}$ molecules/cm².⁵

Solymsi and Bugyi⁸ studied C₂N₂ on Rh(111) with LEED, AES, EELS, and TPD. They detected four C₂N₂ desorption peaks at 380 K (α), 610 K (β_1), 680 K (β_2), and 740 K (γ) from thermal desorption of C₂N₂ adsorbed on Rh(111) at 300 K. The weakly bonded α state was attributed to molecularly adsorbed C₂N₂, while the β and γ states were ascribed to the associative desorption of CN. Nitrogen was observed to desorb at 800 and 850 K, indicating fission of the C–N bond on Rh(111). Following adsorption of C₂N₂ at 110 K, two additional C₂N₂ peaks at 150 K (α_1) and 310 K (α_2) were detected. The saturation coverage of C₂N₂ at 300 K was estimated to be 6.8×10^{14} molecules/cm².

The reaction of CH₃NH₂ on single-crystal metal surfaces has been studied on Pt(111),¹ Pt(100),¹⁷ Ni(111),^{18,19} Ni(100),^{19,20} Cr(111) and Cr(100),¹⁹ Mo(100),²¹ and W(100).²² Methylamine dehydrogenates on all the surfaces studied between 300 and 500 K, and no CH₃NH₂ desorbs intact above 400 K. The reactivity of the C–N bond in CH₃NH₂ also varies greatly on the surfaces studied: it is *completely nondissociative* on Pt(111) (forming HCN and C₂N₂), partially dissociative on Pt(100) and Mo(100) (forming HCN, N₂, and surface carbon), and *completely dissociative* on Ni(111), Ni(100), and W(100) (producing only N₂ and surface carbon).

Hwang, Seebauer, and Schmidt¹ studied the decomposition of CH₃NH₂ on Pt(111) using TPD and AES. Thermal desorption following adsorption at 300 K produces C₂N₂, H₂, and HCN as the major products with the saturated surface producing approximately 4 times more C₂N₂ than HCN. HCN desorbs as two major peaks at 480 and 520 K while C₂N₂ desorbs as several peaks (β and γ states of C₂N₂ in C₂N₂ adsorption on Pt(111)) between 700 and 1200 K. No significant C–N bond scission or nitrogen desorption was observed. The saturation density at 300 K was estimated to be $(3 \pm 1) \times 10^{14}$ molecules/cm². Adsorption at 100 K produces a CH₃NH₂ second monolayer peak at 230 K which saturates at ~ 1 langmuir (1 langmuir = 10⁻⁶ Torr-s) and a CH₃NH₂ multilayer peak at 134 K.

Experimental Section

Experiments were performed in a stainless steel vacuum system equipped with a quadrupole mass spectrometer for gas analysis and TPD and an Auger electron spectrometer (AES) to determine surface cleanliness and measure adsorbate coverages. The base pressure of the system was typically 3×10^{-10} Torr. The Rh(111) crystal was a disk of ~ 0.8 cm diameter which was oriented within 0.5° of (111) and heated to 1750 K by electron bombardment for cleaning and heated resistively to 1300 K for TPD. The crystal was cleaned by heating to 1750 K under vacuum and to 1300 K in oxygen until no contamination peaks were evident in AES.

Heating rates in TPD were typically 22 K/s, although the heating rate decreased at high temperature and was ~ 16 K/s at 1000 K. In the 100 K adsorption experiments, a heating rate of ~ 10 K/s was used for crystal temperature below 500 K to resolve low-temperature multilayer desorption peaks which are usually narrow. The temperature of the crystal was monitored with a W–Re thermocouple and is regarded as accurate to within ± 5 K near 300 K and ± 20 K near 1000 K. The temperature versus time was recorded in all TPD spectra to determine temperatures. All TPD spectra were stored digitally, and peak area calculation and background and cracking pattern subtractions were performed on a microcomputer.

Yields of desorption products from TPD experiments were calibrated against CO (assuming a CO saturation density of 1

$\times 10^{15}$ molecules/cm² on Rh(111) at 300 K,²³ C₂N₂ (3×10^{14} molecules/cm² on Pt(111) at 300 K,^{2,5}), and H₂ (8×10^{14} molecules/cm² on Rh(111) at 100 K²⁴). The pumping speed and the mass spectrometer sensitivity of N₂ are assumed to be the same as those of CO.

The AES N(379 eV)/Rh(202 eV) peak ratio from saturation coverage of C₂N₂ and CH₃NH₂ was calibrated against that from a saturation coverage of NO on Rh(111) at 100 K assuming a saturation density of 1.1×10^{15} NO molecules/cm².²⁵ Comparison of O(505 eV)/Rh(202 eV) AES ratios of CO (0.72 ± 0.02) and NO (0.75 ± 0.03) indicates that the ratio is consistent with the assumed coverages. Care was used in AES calibration to minimize cracking and desorption by using low beam currents and short exposure times and by showing that signals did not exhibit large time dependences.

Cyanogen (98.5+%, Matheson) and methylamine (98.5+%, Linde) were used without further purification. Adsorbates were admitted through a leak valve into the vacuum system at 0.5 to 5×10^{-8} Torr for specified times to attain a desired exposure. CO (99.99%), O₂ (99.98%), and H₂ (99.9995%) were obtained from Matheson and used without further purification for sample cleaning and calibration of TPD areas.

Results

1. C₂N₂. Figure 1 shows TPD spectra of all species observed following exposure to 10 langmuirs of C₂N₂ at 300 K. The two major products detected were C₂N₂ and N₂. A small amount of CO due to background adsorption was also detected, but its TPD peak area was less than 2% of C₂N₂. Total pressure TPD (Figure 1) confirms that C₂N₂ and N₂ were the only major products. TPD experiments in which the crystal was heated to 1400 K were also performed but no desorption above 1000 K was detected.

Figure 2 shows desorption spectra of (a) C₂N₂ and (b) N₂ from C₂N₂ exposures indicated at 300 K. At very low C₂N₂ coverages, C₂N₂ desorbs as a single peak at ~ 820 K (γ). The small, broad peak at ~ 350 K was attributed to desorption from heating leads. At higher coverages, another peak at ~ 750 K (β_2) grows in and shifts downward with increasing coverage as expected for second-order desorption kinetics. Above 1.5 langmuirs, two additional peaks at 380 K (α_4) and 680 K (β_1) appear and become the dominant peaks at saturation (~ 20 langmuirs).

Nitrogen desorption from C₂N₂ exposures (Figure 2b) starts as a broad peak at ~ 820 K and a shoulder at ~ 710 K. This peak shifts upward with increasing coverage and saturates at ~ 10 langmuirs. The small peak at ~ 510 K is attributed to CO desorption from background CO since it does not appear on the $m/e = 14$ spectrum (Figure 1). The two small shoulders at ~ 380 and ~ 680 K observed at higher exposures are due to cracking of C₂N₂ in the mass spectrometer.

Figure 3 shows (a) the total pressure (ion gauge) in TPD experiments and (b) the TPD yield for C₂N₂ ($m/e = 52$) and N₂ ($m/e = 28$). Figure 3a indicates that at lower coverages (< 1 langmuir), most C₂N₂ dissociates to form N₂ and surface carbon residue while at higher coverages (> 1 langmuir), most C₂N₂ molecules adsorbed desorb without C–N bond scission. In fact, at very low coverages (< 0.2 langmuir), no C₂N₂ desorption was detected (Figure 3b): all C₂N₂ molecules adsorbed decompose completely to N₂ and adsorbed carbon residue. This observation is consistent with the results of Solymsi and Bugyi.⁸

Similar experiments were carried out with adsorption of C₂N₂ at 100 K. Above 400 K, the spectra appear similar to those obtained following adsorption at 300 K. Below 400 K, at least three additional C₂N₂ desorption peaks at 115 K (α_1), 155 K (α_2), and 310 K (α_3) were detected. At very low coverages (< 4 langmuirs), C₂N₂ desorbs as a small first-order peak at ~ 155 K (α_2) and a broad peak which was attributed to desorption from heating leads between 250 and 450 K. The α_2 state saturates at

(17) Thomas, P. A.; Masel, R. I. *J. Vac. Sci. Technol. A* **1987**, *5*, 1106.

(18) Chorkendorff, J.; Russell, Jr., J. N.; Yates, Jr., J. T. *J. Chem. Phys.* **1987**, *86*, 4692.

(19) Baca, A. G.; Schulz, M. A.; Shirley, D. A. *J. Chem. Phys.* **1985**, *83*, 6001.

(20) Schoofs, G. R.; Benziger, J. B. *J. Phys. Chem.* **1988**, *92*, 741.

(21) Walker, B. W.; Stair, P. C. *Surf. Sci.* **1981**, *103*, 315.

(22) Pearlstine, K. A.; Friend, C. M. *J. Am. Chem. Soc.* **1986**, *108*, 5842.

(23) Castner, D. G.; Sexton, B. A.; Somorjai, G. A. *Surf. Sci.* **1978**, *71*, 519.

(24) Yates, Jr., J. T.; Thiel, P. A.; Weinberg, W. H. *Surf. Sci.* **1979**, *84*, 427.

(25) Root, T. W.; Schmidt, L. D.; Fisher, G. B. *Surf. Sci.* **1983**, *134*, 30.

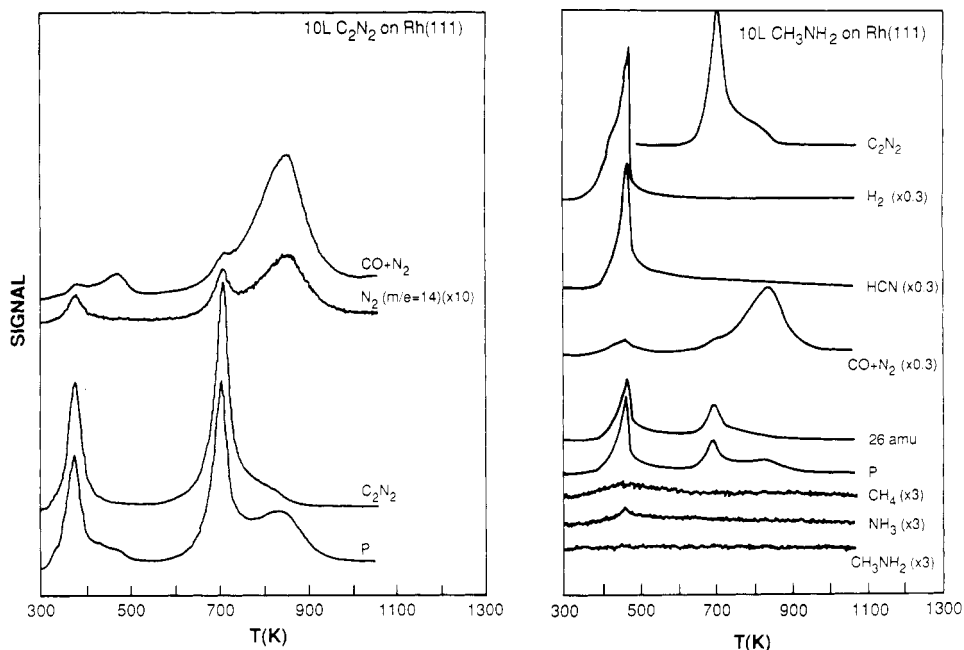


Figure 1. Left panel shows TPD spectra of C_2N_2 and its reaction products on Rh(111) following 10 langmuirs C_2N_2 exposure at 300 K. Total pressure response (from ion gauge) indicates that C_2N_2 and N_2 are the only major products. In most spectra shown, the heating rate β was ~ 22 K/s unless otherwise specified. Right panel shows TPD spectra of CH_3NH_2 and its reaction products on Rh(111) following 10 langmuirs CH_3NH_2 exposure at 300 K. Total pressure response indicates that C_2N_2 , H_2 , HCN, and N_2 are the only major products. In the 26 amu spectrum, the peak at ~ 440 K is attributed to mass spectrometer cracking fragment of HCN and the peak at ~ 680 K of C_2N_2 . CH_4 and NH_3 peak areas were no more than a few percent of C_2N_2 . No desorption of the CH_3NH_2 parent molecule was detected.

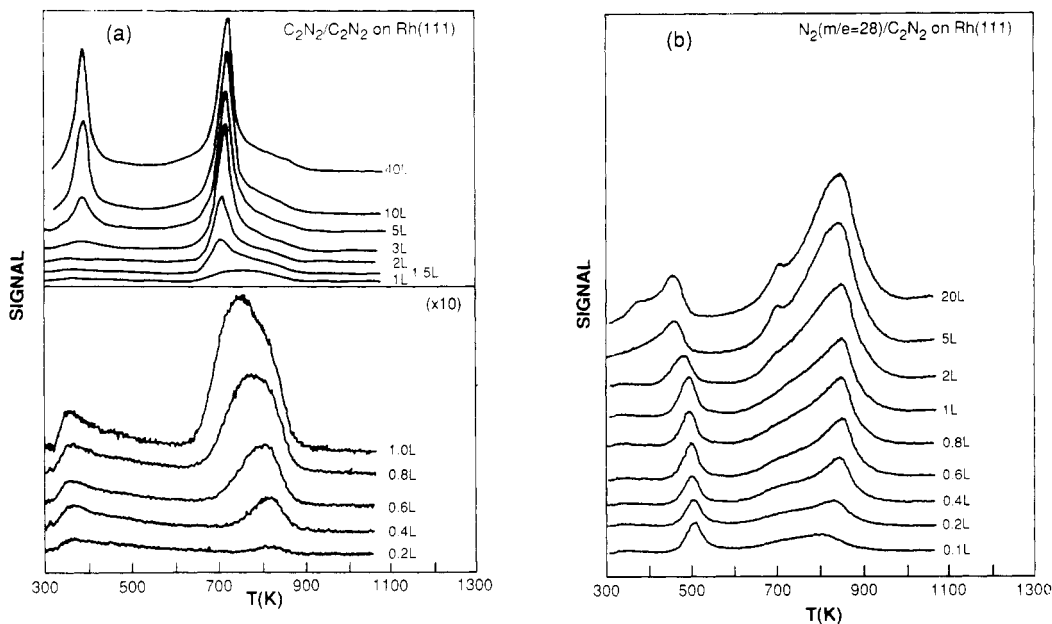


Figure 2. TPD spectra of (a) C_2N_2 and (b) N_2 on Rh(111) following indicated C_2N_2 exposures at 300 K.

~ 12 langmuirs. At higher coverages (>4 langmuirs), two peaks at 310 K (α_3) and 365 K (α_4) appear. Both peaks show no significant shift in peak temperature and saturate at ~ 10 langmuirs. The α_4 peak is assumed to be the same peak as the 380 K peak observed with room temperature adsorption. C_2N_2 exposures higher than 12 langmuirs produce an additional peak at ~ 115 K (α_1) which is a multilayer peak because it does not saturate by 40 langmuirs.

2. CH_3NH_2 . Since CH_3NH_2 adsorbs strongly on the walls of the vacuum system, pumping down from 5×10^{-8} Torr (where most dosing was carried out) to the system base pressure usually takes ~ 30 min. Actual exposures were therefore difficult to estimate and only nominal exposures are cited for CH_3NH_2 experiments. In some cases, especially at low exposures, actual exposure may be higher than the nominal exposure by up to a factor of 3.

Figure 1 shows TPD spectra of all species observed following exposure to 10 langmuirs of CH_3NH_2 at 300 K. The major products detected were C_2N_2 , HCN, H_2 , and N_2 . Desorption of CH_4 and NH_3 were no more than a few percent of C_2N_2 and no desorption of the CH_3NH_2 parent molecule was detected. The $m/e = 26$ spectrum shows the cracking pattern of CN^+ from both HCN and C_2N_2 . The total pressure shows no major desorption peaks other than the products observed. TPD experiments with the crystal ramped to 1300 K revealed no additional peaks above 1000 K.

Figure 4 shows TPD spectra of (a) C_2N_2 , (b) HCN, (c) H_2 , and (d) N_2 from indicated CH_3NH_2 exposures at 300 K. At low CH_3NH_2 exposures, cyanogen desorption from CH_3NH_2 (Figure 4a) is similar to that from C_2N_2 exposures in that both start with a single peak at ~ 820 K (γ) and an additional peak at ~ 750 K (β_2) detected at <1 langmuir. However, the small broad peak

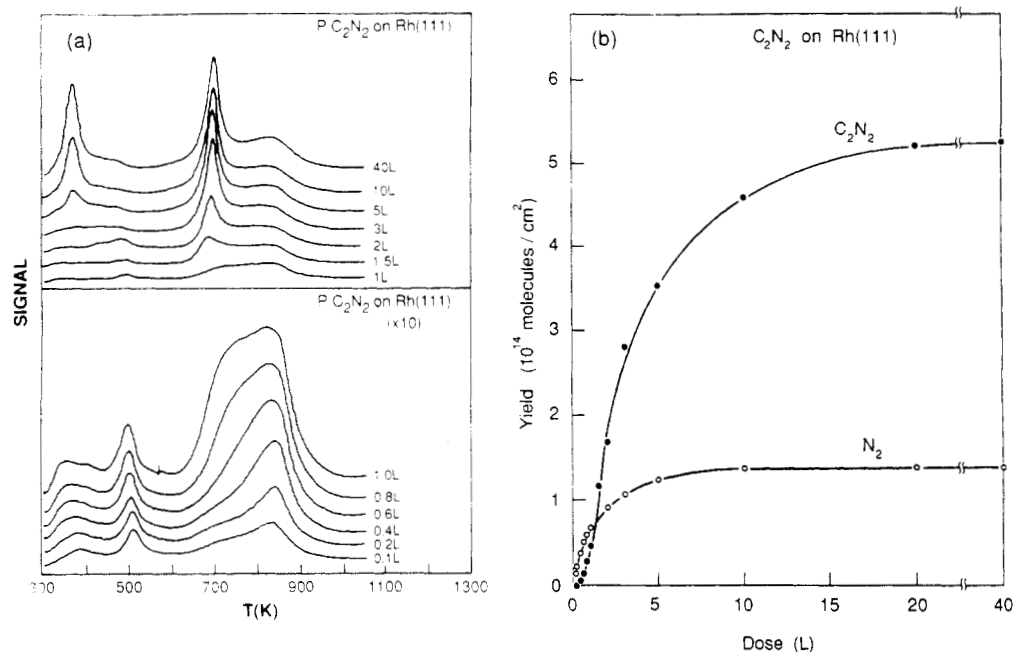


Figure 3. (a) Total pressure response (from ion gauge) and (b) product yields of C_2N_2 and N_2 as a function of C_2N_2 exposure at 300 K. Product yields were obtained from TPD peak areas with calibration discussed in the text.

at ~ 350 K in the spectra from C_2N_2 exposure is missing in the spectra from CH_3NH_2 . This is consistent with our assignment of this peak as arising from molecularly adsorbed C_2N_2 on the heating leads. At higher coverages (>1 langmuir), an additional peak at ~ 680 K (β_1) grows in and becomes the dominant peak at saturation (~ 10 langmuirs).

Comparison of the C_2N_2 desorption spectra from C_2N_2 and CH_3NH_2 therefore shows that C_2N_2 desorbs from these two adsorbates identically above 500 K as expected if no additional species are present. It is noted, however, that the β_1 peak from CH_3NH_2 adsorption at saturation is smaller than that from C_2N_2 . This is due to a lower coverage of CH_3NH_2 than C_2N_2 at room temperature. The C_2N_2 peak at 380 K (α) from C_2N_2 exposure is missing in the spectra from CH_3NH_2 adsorption (Figure 4a). This is consistent with the assignment of that peak to molecularly adsorbed C_2N_2 .

At low coverages (<0.5 langmuir) no HCN desorption was observed except for the two small broad peaks at 580 and 700 K (Figure 4b), both attributed to desorption from heating leads. At 0.5 langmuir, HCN desorption emerges at ~ 430 K, comparable to HCN desorption temperature on Pt(111) and Pd(111).^{26,27} This peak shifts upward with increasing exposure (to ~ 450 K at saturation) and saturates at ~ 10 langmuirs.

The desorption of hydrogen (Figure 4c) shows two unresolved narrow peaks at 420 and 430 K and two broader peaks at 370 and 405 K at 0.5 langmuir. With increasing exposure, all four peaks shift upward in peak temperature but only the three high-temperature peaks at 405, 420, and 430 K grow with exposure while the peak at 370 K shrinks to $\sim 1/3$ of its original height at saturation. Since hydrogen adsorbed on Rh(111) at room temperature desorbs at ~ 370 K at low coverages,²⁸ the 370 K peak may arise from very low exposures of CH_3NH_2 molecules which dehydrogenate partially upon adsorption at room temperature. The decreasing intensity of this peak at high exposures shows that high densities of CH_3NH_2 block sites for low-temperature desorption.

Comparison of the N_2 desorption spectra from CH_3NH_2 (Figure 6d) and C_2N_2 (Figure 2b) indicates that they follow the same decomposition path: scission of C-N bonds followed by recom-

TABLE I: Yields^a of Desorption Products from Saturation Coverages of C_2N_2 and CH_3NH_2 on Rh(111) and Pt(111) [1,2] at 300 K

product	C_2N_2		CH_3NH_2	
	Pt(111)	Rh(111)	Pt(111)	Rh(111)
monolayer	3.0×10^{14}	6.7×10^{14}	4.0×10^{14}	8.2×10^{14}
C_2N_2	3.0	5.3	1.8	1.6
N_2	<0.1	1.4	<0.1	1.8
HCN	<0.1	<0.1	0.4	1.4
H_2	<0.1	<0.1	<i>b</i>	13.9

^aAmounts were obtained from TPD peak areas with calibrations discussed in text. All yields are in molecules/cm². ^bHydrogen yield from CH_3NH_2 adsorption on Pt(111) was not calibrated in ref 1.

bination of surface N atoms. The nitrogen desorption spectra from CH_3NH_2 show a smaller peak at 680 K (due to C_2N_2), indicative of less C_2N_2 produced from CH_3NH_2 than from C_2N_2 . Comparison of the nitrogen TPD peak area at saturation shows that CH_3NH_2 produces 29% more N_2 than C_2N_2 . The small peak at 450 K in the CH_3NH_2 spectra is attributed to cracking pattern of HCN (possibly H_2CN^+) in the mass spectrometer.

Thermal desorption of CH_3NH_2 adsorbed on Rh(111) at 100 K produces similar desorption spectra above 300 K (data not shown). Below 300 K, only one CH_3NH_2 multilayer peak is observed. This peak starts at ~ 120 K, shifts upward with increasing exposure, and does not saturate. In addition to the hydrogen desorption peaks observed in the 300 K experiments, a H_2 peak at ~ 320 K was observed. This peak is at least 2 times bigger than the 370 K peak and should arise from partial dehydrogenation of CH_3NH_2 to the H_2CN species near room temperature.

3. Adsorbate Coverages and Sticking Coefficients. Yields of desorption products from saturation coverages of C_2N_2 and CH_3NH_2 on Rh(111) at 300 K were calibrated against CO (for N_2)²³ and H_2 on Rh(111)²⁴ and C_2N_2 on Pt(111)²⁵ and are listed on Table I together with those on Pt(111) from our previous work.^{1,2} The saturation densities of C_2N_2 and CH_3NH_2 (based on N atoms) on Rh(111) at 300 K were then estimated to be 6.7×10^{14} and 8.2×10^{14} molecules/cm², about a factor of 2 higher than those on Pt(111).

The hydrogen balance in Table I from CH_3NH_2 adsorption shows clearly a large hydrogen deficiency ($\sim 29\%$); this may arise from desorption of the adsorbed H atoms from dehydrogenation of very low coverage of CH_3NH_2 molecules upon adsorption at 300 K as evidenced by the 320 K hydrogen desorption peak

(26) Hagans, P. L.; Guo, X.; Chorkendorff, I.; Winkler, A.; Siddiqui, H.; Yates, Jr., J. T. *Surf. Sci.* **1988**, *203*, 1.

(27) Guo, X.; Hoffman, A.; Hagans, P. L.; Yates, Jr., J. T., submitted for publication in *J. Am. Chem. Soc.*

(28) Hwang, S. Y. Ph.D. Thesis, University of Minnesota, 1988.

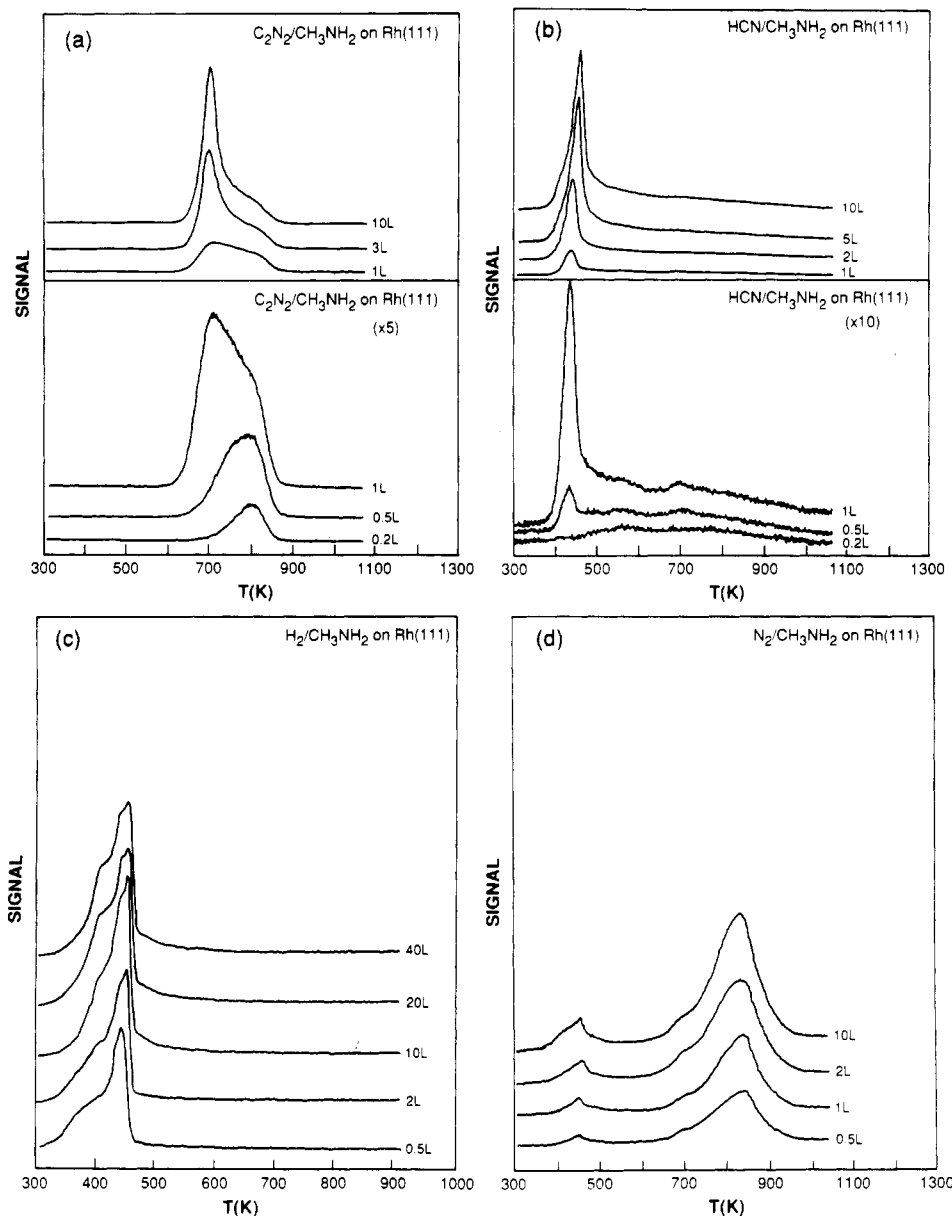


Figure 4. TPD spectra of (a) C_2N_2 , (b) HCN, (c) H_2 , and (d) N_2 on Rh(111) following indicated CH_3NH_2 exposures at 300 K.

observed in the experiments with CH_3NH_2 adsorption at 100 K. Table I also indicates that 20% of C_2N_2 and 44% of CH_3NH_2 molecules adsorbed decomposed to nitrogen and surface carbon residues while no C-N bond scission and nitrogen desorption were observed from thermal desorption of these two molecules on Pt(111).^{1,2,4,5}

Figure 5 shows AES spectra of (a) a clean Rh(111) surface and Rh(111) exposed to (b) 40 langmuirs of CO, (c) 40 langmuirs of NO, (d) 40 langmuirs of C_2N_2 , and (e) 40 langmuirs of CH_3NH_2 . The AES N(379 eV)/Rh(202 eV) peak ratio from a saturation coverage of C_2N_2 (Figure 7d, 0.22 ± 0.01) is calibrated with that of an NO-saturated surface (Figure 5c, 0.21 ± 0.01); a saturation density of $(6.4 \pm 0.3) \times 10^{14}$ molecules/cm² was obtained, comparable to the value obtained from calibration of TPD peak areas. Similar calibration for a CH_3NH_2 saturated surface (Figure 5e), however, yields a saturation density of $(1.5 \pm 0.1) \times 10^{15}$ molecules/cm² at 300 K, 85% higher than the value obtained from TPD experiments. This may arise from cracking of the adsorbed species induced by the electron beam although a very low beam current was used.

The initial sticking coefficient from the slope of the $C_2N_2 + N_2$ desorption curve in Figure 3a gives $S_0 = 0.2$ for C_2N_2 . Although the initial sticking coefficient of CH_3NH_2 is difficult to measure due to the difficulties in determining exact CH_3NH_2

exposures, S_0 for CH_3NH_2 is estimated to be ~ 0.3 from the 0.5 and 1 langmuir spectra in Figure 4.

Discussion

1. C_2N_2 . Figure 6a indicates our interpretation of the steps in C_2N_2 decomposition on Rh(111). Shown in the figure are TPD peak temperatures for each product and possible surface species. All C_2N_2 molecules adsorbed on Rh(111) either desorb intact from associative states at 115 (multilayer), 155, 310, and 380 K and dissociative states at 680, 750, and 820 K or decompose (from CN) at 820 K to nitrogen and surface carbon residues. Figure 3b indicates that at least 60% of the first langmuir of C_2N_2 adsorbed on Rh(111) at 300 K decomposes to N_2 and surface carbon. This is in sharp contrast with Pt(111) on which no decomposition was observed.^{2,4,5} However, the decomposition (revealed by desorption of N_2) saturates below 10 langmuirs while C_2N_2 desorption continues to grow until it saturates at ~ 40 langmuirs (where 80% of C_2N_2 molecules desorb intact).

Comparison of the results in this study with those of Solymosi and Bugyi⁸ indicates that they are generally comparable, although some differences are noted in both relative amounts and TPD spectra. Both studies observe C_2N_2 and N_2 as the only products and estimate a saturation density of $\sim 6.8 \times 10^{14}$ C_2N_2 molecules/cm². N_2 is found to be the major product at low coverages

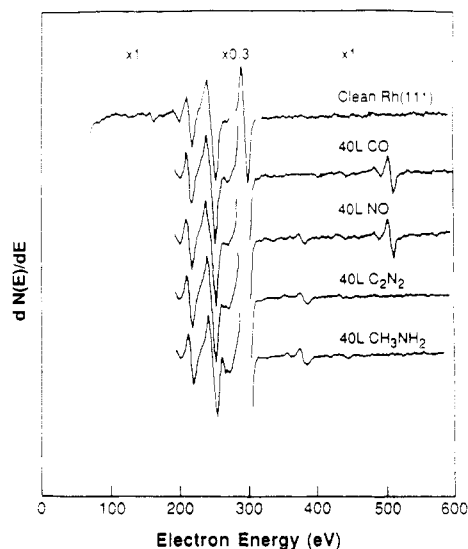


Figure 5. AES spectrum of (a) clean Rh(111) and Rh(111) exposed to (b) 40 langmuirs of CO, (c) 40 langmuirs of NO, (d) 40 langmuirs of C_2N_2 , and (e) 40 langmuirs of CH_3NH_2 .

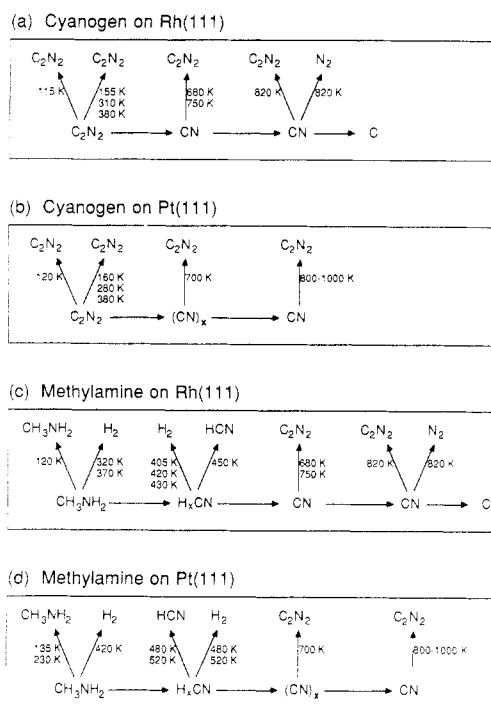


Figure 6. Proposed reaction path of C_2N_2 on (a) Rh(111) and (b) Pt(111),^{2,28} and CH_3NH_2 on (c) Rh(111) and (d) Pt(111).¹ Shown in the figure are TPD peak temperatures of each product and possible surface species.

in both studies, although desorption of C_2N_2 is always less than that of N_2 in Solymosi and Bugyi while we observe the desorption of C_2N_2 to be 4 times larger than that of N_2 at saturation. This discrepancy should arise mainly from calibration of product yields which was not stated in ref 8.

Most of the C_2N_2 desorption peaks, namely the five peaks at 155, 310, 380, 680, and 750 K, are reproduced in the two studies while the two peaks at 120 and 820 K observed in this study are not reported previously⁸ and the 610 K peak observed in ref 8 is not found in the C_2N_2 spectra in Figure 2a. The reason why the peaks at 120 and 820 K were not reported in ref 8 should be straightforward: the adsorption temperature in ref 8 (110 K) was too high to observe the 120 K peak and the presence of the 820 K is difficult to detect since the peak is small and it overlaps strongly with the other peak at 750 K at high exposures (Figure 2a). However, the absence of the C_2N_2 peak at 610 K which was

observed by Solymosi and Bugyi is not understood. As for the desorption of N_2 , Solymosi and Bugyi⁸ reported two peaks of comparable sizes at 800 and 850 K while only one major N_2 peak at 820 K and a much smaller shoulder at ~ 710 K were observed in this study.

Comparison of the decomposition paths of C_2N_2 on Rh(111) and Pt(111)^{2,28} indicates that they are similar up to ~ 800 K (Figure 6a,b). Adsorption of C_2N_2 at low temperature produces at least four C_2N_2 desorption peaks below 400 K on both surfaces with the peak near 120 K arising from the C_2N_2 multilayer (ice). At lower coverages, the C-C bond in C_2N_2 dissociates on both surfaces leaving adsorbed CN which desorbs as C_2N_2 through recombination in at least two peaks starting at ~ 680 K. Above ~ 780 K, however, a reaction channel which breaks the C-N bond to form N_2 and surface carbon (γ state) opens up on Rh but not on Pt. This channel competes with the desorption of CN as C_2N_2 and results in depletion of surface CN and the absence of the higher temperature states of C_2N_2 on Rh(111).

Comparison of the C_2N_2 decomposition on Rh(111) and Pt(111) with that on other transition-metal surfaces²⁻¹⁶ reveals some important differences in the reactivity of the C-N bond in C_2N_2 on these metals. The C-N bond is fully broken on Ni (producing only N_2), partially broken on Ru¹⁶ and Rh (C_2N_2 and N_2 desorb), and not broken on Pt, Cu, Pd, and Ag (only C_2N_2 desorbs); the C-C bond is cleaved on Pt, Cu, and Pd but not on Ag. On Ru(100), C_2N_2 desorbs in three peaks at 470 (α), 600 (β), and 700 K (γ) and a small shoulder at 750 K.¹⁶ The γ state is the dominant species in the adlayer on Ru(100) at room temperature with a saturation density equivalent to $\sim 2.5 \times 10^{14}$ cyanogen molecules/cm²; 85% decomposes to carbon and nitrogen. From the relative amounts and the desorption temperature of N_2 from adsorption of C_2N_2 on Rh(111) and Ru(100), it is clear that Ru is more reactive toward the C-N bond in C_2N_2 than is Rh.

Although the C-N bond in C_2N_2 is not broken on Pt, Cu, or Pd, comparison of the C_2N_2 desorption temperatures from the β states of C_2N_2 (recombination of the nitrile group) should be indicative of the reactivity of the C-N bond because higher desorption temperature suggests lower reactivity. Since the β states of C_2N_2 desorption start with a peak between 530 and 560 K on Pd surfaces,^{9,10} between 670 and 700 K on Pt²⁻⁷ and between 815 and 850 K on Cu,¹²⁻¹⁴ it appears that the reactivity of the C-N bond on these metals should follow the order Pd > Pt > Cu. In summary, the reactivities of the C-N bond in C_2N_2 appear to follow the order of Ni > Ru > Rh > Pd > Pt > Cu > Ag.

2. CH_3NH_2 . Figure 6c shows our interpretation of the decomposition paths of CH_3NH_2 on Rh(111). All CH_3NH_2 molecules on Rh(111) either desorb intact at 120 K (multilayer) or dehydrogenate to H_2 , HCN, and C_2N_2 above 300 K. No CH_3NH_2 desorption near 250 K (second CH_3NH_2 monolayer) was observed, although peaks at similar temperatures were reported on Pt(111),¹ Pt(100),¹⁶ Ni(111),¹⁷ Ni(100),¹⁹ and W(100).²¹ Some of the carbon formed on Rh(111) remains on the surface after TPD at 1300 K.

Adsorption of CH_3NH_2 on Rh(111) should be through the lone pair of electrons on the N atom as on Ni and Cr.¹⁹ At very low coverages, all the CH_3NH_2 molecules adsorbed dehydrogenate completely by 460 K to leave surface nitrile groups (CN) which desorb as C_2N_2 through recombination and as N_2 through scission of the C-N bond at ~ 820 K. No desorption of HCN was observed for CH_3NH_2 exposures below 0.5 langmuir. Dehydrogenation of CH_3NH_2 should begin near 300 K, as evidenced by the hydrogen desorption peak at 320 K. Thus, it appears that CH_3NH_2 molecules are partially dehydrogenated to some H_xCN species upon adsorption on Rh(111) near room temperature.

In contrast, Baca, Schulz, and Shirley¹⁹ reported the presence of molecular adsorption of CH_3NH_2 on surfaces of Cr and Ni at 300 K, although a substantial amount of dissociation on chromium also occurred. Although the desorption of CH_3NH_2 is not complete until ~ 350 K (with peak at ~ 250 K) on Pt(100),¹⁷ Ni(100),²⁰ or W(100),²² the onset of the hydrogen desorption near 300 K on these surfaces suggests that partial dehydrogenation of CH_3NH_2 starts near room temperature. It thus appears that

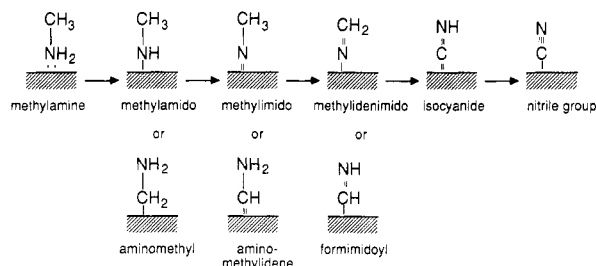


Figure 7. A possible dehydrogenation path of adsorbed CH_3NH_2 molecule to H_xCN and then to CN species with some of the possible surface H_xCN species. Complete dehydrogenation of adsorbed CH_3NH_2 molecule to surface CN occurs within a narrow temperature range between 300 and 460 K on Rh(111) and a somewhat wider range between ~ 330 and 600 K on Pt(111).¹

CH_3NH_2 molecules begin to dehydrogenate between 300 and 350 K on all transition-metal surfaces studied so far.

The nature of the H_xCN species is not clear; they can be any of the possible surface species shown in Figure 7. Since CH_3NH_2 dehydrogenates completely to CN between 300 and 460 K, more than one of these species probably exist on the surface at different temperatures. Figure 7 shows a possible decomposition path of CH_3NH_2 dehydrogenation to CN. Determination of which of the species in Figure 7 actually exist at a certain temperature is difficult even with EELS or isotope-labeled adsorbates because complete dehydrogenation occurs in at least four steps (four H_2 desorption peaks) within a small temperature range between 300 and 460 K. As a comparison, Yates and co-workers¹⁸ studied the dehydrogenation of CH_3NH_2 on Ni(111) by TPD with deuterated CH_3NH_2 molecules and found that the CH_3NH_2 decomposition takes place through both ends of the molecule, initially with a slight rate preference at the C end. On Pt(111), comparison of the CH_3NH_2 and CH_3NO_2 decomposition suggests that CH_3NH_2 probably dehydrogenates first at the N end.^{1,2}

Since the methoxy ($-\text{O}-\text{CH}_3$) and the ethylidyne ($\equiv\text{C}-\text{CH}_3$) species should have similar molecular structures to the H_xCN species (e.g., methylimido = $\text{N}-\text{CH}_3$) in this study, and their thermal stabilities on surfaces of transition metals have been studied extensively,²⁹⁻³⁵ it is instructive to compare the decomposition of the H_xCN species with that of methoxy and ethylidyne. The formation and stability of the methoxy species on transition-metal surfaces have been studied extensively by EELS and TPD of CH_3OH adsorption at low temperatures.²⁹⁻³¹ On Pt(111), adsorption of CH_3OH at low temperature does not produce any detectable stable methoxy species^{29,30} unless the surface is preadsorbed with a $p(2\times 2)$ layer of adsorbed oxygen atoms.²⁹ In this case the OCH_3 species is detected at ~ 170 K but decomposes completely to adsorbed CO and H by 300 K. On Rh(111), methoxy can also be produced by adsorption of methanol, although methoxy decomposes to adsorbed CO and H completely by 220 K on Rh(111).³¹

Upon adsorption of C_2H_4 on Pt(111) at low temperatures, the ethylidyne species is found to be formed at ~ 280 K and remains

stable up to ~ 440 K above which it dehydrogenates in several H_2 peaks between 490 and 710 K to leave surface carbon residues.^{32,33} On Rh(111), the formation of a stable $c(4\times 2)$ overlayer of ethylidyne species by adsorption of C_2H_4 at 300 K has been well studied.^{34,35} The ethylidyne species is stable on Rh(111) up to ~ 400 K above which it dehydrogenates to surface carbon in a single H_2 peak at 440 K followed by a continuous H_2 evolution band up to 750 K.³⁴

Since the H_xCN species from CH_3NH_2 adsorption dehydrogenates to C-N between 320 and 600 K on Pt(111)¹ and between 300 and 460 K on Rh(111), comparison of the onset of decomposition of the three species on Pt(111) and Rh(111) indicates that the stabilities of these species follow the order $\text{CCH}_3 > \text{H}_x\text{CN} > \text{OCH}_3$ on both surfaces. It is also noted that Rh is more reactive than Pt for CCH_3 and H_xCN while the reverse is true for the OCH_3 species. However, it should also be noted that dehydrogenation of H_xCN and OCH_3 does not involve cleavage of C-N or C-O²⁹⁻³¹ bond while that of CCH_3 involves breaking of the C-C bond.³²⁻³⁵

Following the complete dehydrogenation of CH_3NH_2 to CN between 300 and 460 K, the only species remaining on the surface is CN which follows the decomposition path of C_2N_2 : desorption of C_2N_2 at 680 K (β_1), 750 K (β_2), and 820 K (γ) and N_2 at 820 K. The β_1 state of C_2N_2 from CH_3NH_2 adsorption is smaller than that from C_2N_2 exposure simply because of a lower saturation CN coverage from CH_3NH_2 .

Comparison of the decomposition path of CH_3NH_2 on Rh(111) and Pt(111)¹ suggests that the major difference between these two metals is their ability to break the C-N bond (Figure 6c,d). The Rh surface is capable of breaking $\sim 40\%$ of the C-N bond while no C-N bond scission is observed on Pt(111). Complete dehydrogenation of adsorbed CH_3NH_2 molecules to CN takes place at a lower temperature and over a narrower range on Rh(111) than on Pt(111). In summary, Rh appears to be more reactive than Pt to all the bonds in CH_3NH_2 (including C-N, C-H, and N-H).

Summary

Adsorption of C_2N_2 on Rh(111) at 300 K produces mostly C_2N_2 (80%) while a significant amount of N_2 (20%) from scission of the C-N bond is also observed. C_2N_2 desorption spectra exhibit at least four peaks while the N_2 spectra show only a single peak at 820 K. From a comparison of the C_2N_2 desorption on several metals, the reactivity of the C-N bond in C_2N_2 on transition-metal surfaces appears to follow the order $\text{Ni} > \text{Ru} > \text{Pd} > \text{Pt} > \text{Cu} > \text{Ag}$.

CH_3NH_2 dehydrogenates on Rh(111) near room temperature to several surface H_xCN species which then dehydrogenate completely between 350 and 460 K to CN to desorb as C_2N_2 and N_2 . The decomposition path of CH_3NH_2 above ~ 500 K is therefore identical with that from C_2N_2 exposure except for a lower CN coverage from CH_3NH_2 . Below 0.5 langmuir, all CH_3NH_2 dehydrogenates completely to CN by 460 K; no desorption of HCN was observed. At higher coverages, increasing HCN was detected such that at saturation, about equal amounts of C_2N_2 , N_2 and HCN were produced. The stability of the H_xCN species from adsorption of CH_3NH_2 appears to be between that of the methoxy (OCH_3 , from CH_3OH exposures) and the ethylidyne (CCH_3 , from C_2H_4) species on Rh(111) and Pt(111).

Registry No. Rh, 7440-16-6; C_2N_2 , 460-19-5; CH_3NH_2 , 74-89-5; N_2 , 7727-37-9.

(29) Sexton, B. A. *Surf. Sci.* **1981**, *102*, 271.

(30) Ehlers, D. H.; Spitzer, A.; Luth, H. *Surf. Sci.* **1985**, *160*, 57.

(31) Solymosi, F.; Berko, A.; Tarnóczy, T. I. *Surf. Sci.* **1984**, *141*, 533.

(32) Salmerón, M.; Somorjai, G. A. *J. Phys. Chem.* **1982**, *86*, 341.

(33) Creighton, J. R.; White, J. M. *Surf. Sci.* **1983**, *129*, 327.

(34) Dubois, L. H.; Castner, D. G.; Somorjai, G. A. *J. Chem. Phys.* **1980**, *72*, 5234.

(35) Koestner, R. J.; Van Hove, M. A.; Somorjai, G. A. *Surf. Sci.* **1982**, *121*, 321.